

Unusual Assembly of Small Organic Building Molecules in Common Solvent

Huisheng Peng*

Los Alamos National Laboratory, Los Alamos, New Mexico 87545

Received: March 22, 2007; In Final Form: May 29, 2007

During the process of self-association, reaching a thermodynamic equilibrium state in dilute solution is usually very fast, taking at most seconds for small organic (such as surfactants) solutions and hours for polymer solutions. It is very rare that days are necessary for soluble small organic molecules to reach thermodynamic stability in dilute solutions. This work reports such an unusually slow association of two polymerizable organic molecules, $\text{HOOC}(\text{CH}_2)_3\text{CCCC}(\text{CH}_2)_3\text{COOH}$ and $(\text{EtO})_3\text{Si}(\text{CH}_2)_3\text{NH}_2$, in their common solvent. The self-organization process of above complexes spanned several minutes to several days, depending on their concentrations. The morphologies of resultant aggregates, ranging from vesicles to solid spheres and to hollow spheres, were also tunable by varying the molar ratios of two precursors. Enriched functional COOH/NH₂ groups on the aggregate surface can attach various antibodies, which endow the nanoparticles with great potential applications as targeted drug-delivery vehicles. In addition, as-synthesized hybrid aggregates could be further stabilized by either addition reaction of diacetylenic acid or hydrolysis and condensation reactions of 3-aminopropyltriethoxysilane. In particular, the derived polydiacetylenic aggregates demonstrate a thermochromatic property and may be applied as sensing materials. Those novel phenomena, along with the simplicity in the preparation of aggregates, make the system promising in addressing related theoretical problems and practical applications.

Introduction

Engineered nanometer-sized capsules have recently attained widespread interest due to their potential applications in diagnostics, catalysis, therapy, and bioengineering in both aqueous and nonaqueous media.^{1–3} Most successful examples of such nanosystems are vesicles,^{4,5} hollow spheres,^{6,7} and micelles.^{8–10} The advantages of these structures are their small (and usually variable) sizes, high stability, and controlled permeability. Different fabrication methods, such as self-assembly of copolymers and the use of colloidal particles or liposomes as templates, have been explored.^{3,11,12} However, synthesis of such capsules by directed assembly of two polymerizable small organic molecules in their common solvent, followed by polymerization, has not been reported to date.

During the process of self-association, reaching a thermodynamic equilibrium state in dilute solution is usually very fast, taking at most seconds for small organic (such as surfactants) solutions^{13,14} and hours for polymer solutions.¹⁴ We have explored the self-assembly of polymer/surfactant complexes in their common organic solvent, a process factually requiring seconds.^{15,16} It is very rare that days are necessary for soluble small organic molecules to reach thermodynamic stability in dilute solutions. This work reports such an unusually slow association of two polymerizable organic molecules, $\text{HOOC}(\text{CH}_2)_3\text{C}\equiv\text{CC}\equiv\text{C}(\text{CH}_2)_3\text{COOH}$ and $(\text{EtO})_3\text{Si}(\text{CH}_2)_3\text{NH}_2$, in a common organic solvent. The self-organization process of above complexes spanned several minutes to several days, depending on the concentrations. Higher concentrations were conducive to faster association. The morphologies of resultant aggregates, ranging from vesicles to solid spheres and to hollow spheres, were tunable by varying the molar ratios (MR) between 5,7-dodecadienedioic acid and 3-aminopropyltriethoxysilane build-

ing molecules. Enriched functional COOH/NH₂ groups on the aggregate surface can attach various labeled biomolecules, which endows the nanoparticles with great potential applications as targeted drug-delivery vehicles. In addition, as-synthesized hybrid aggregates could be further stabilized by either addition reaction of 5,7-dodecadienedioic acid or hydrolysis and condensation reactions of 3-aminopropyltriethoxysilane. The interesting assembly behavior and manipulability make this system promising in a wide range of research fields and applications.

Experimental Methods

Typical Synthesis of Supramolecular Assemblies (1 mg/mL). 5,7-Dodecadienedioic acid and 3-aminopropyltriethoxysilane were dissolved separately in their common solvent THF. 5,7-dodecadienedioic acid solution was filtered to remove any polymerized impurity prior to use. The aggregates with molar ratios (MR) ranging from 5/1 and 1/1 to 1/2 were prepared by adding the designated amount of 3-aminopropyltriethoxysilane solution (1 mg/mL) to 5,7-dodecadienedioic acid solution (1 mg/mL) dropwise under ultrasonic at room temperature.

Loading and Releasing of α -sexithiophene. A 1 mg sample of α -sexithiophene was added to 10 mL of aggregate solutions (1 mg/mL, MR = 1/1), and the mixture was incubated at room temperature for 1 day. The mixture was then centrifuged to remove the supernatant. The concentrated aggregates were collected by filtration using an aluminum membrane of 20 nm pore diameter. The releasing study was conducted by dissolving the aggregate powder in THF.¹⁷

Loading and Releasing of Aspirin. A 5 mg sample of aspirin was added to 15 mL of vesicle solution (1 mg/mL, MR = 1/2), and the mixture was incubated at room temperature for 1 day. Similarly, the mixture was centrifuged to remove the excessive aspirin. The vesicle powder loaded with aspirin was collected

* Fax: (505) 663-5550. Phone: (505) 663-5552. E-mail: hpeng@lanl.gov.

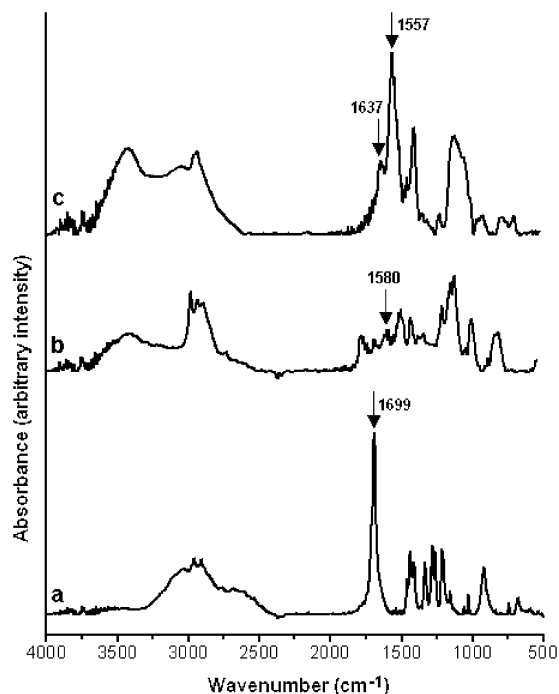


Figure 1. FTIR spectra of (a) pure 5,7-dodecadienedioic acid, (b) pure 3-aminopropyltriethoxysilane, and (c) the complexes of $\text{HOOC}(\text{CH}_2)_3\text{C}\equiv\text{C}(\text{CH}_2)_3\text{COOH}$ and $(\text{EtO})_3\text{Si}(\text{CH}_2)_3\text{NH}_2$ at 1 mg/mL and $\text{MR} = 1/2$.

by filtration using an aluminum membrane of 20 nm pore size. The releasing process of aspirin was followed by UV–vis spectrometer.

Analysis. Dynamic laser light scattering (DLS, Brookhaven 90Plus) was used to measure the hydrodynamic diameter and diameter distribution of the hybrid aggregates. In DLS, the Laplace inversion of a measured intensity-time correlation function $G^{(2)}(t, q)$ in the self-beating mode can result in a line-width distribution $G(\lambda)$. For a pure diffusive relaxation, is related to the translational diffusion coefficient D by $\Gamma/q^2 = D$ or a hydrodynamic radius R_h by $R_h = k_B T / 6\pi\eta D$, where k_B , T , and η are the Boltzmann constant, absolute temperature, and solvent viscosity, respectively. In this study, the aggregate concentrations are low and in the range of 10^{-4} – 10^{-3} g/mL, so the solutions were directly measured without dilution. All the measurements were performed at room temperature with a fixed scattering angle (θ) of 90° .

The IR spectra of the complexes were recorded by a Thermo Nicolet Nexus 670 Fourier transform infrared (FTIR) spectrophotometer with a Smart MIRacle horizontal attenuated total reflectance Ge crystal accessory. The morphologies of the aggregates were characterized using transmission electron microscopy (TEM, JEOL 2010 operated at 120 kV). UV–visible spectra were recorded using a Beckman DU 640B Ultraviolet–visible spectrophotometer.

Results and Discussion

THF is utilized as a common solvent for the two precursors since no aggregation was detected by dynamic light scattering in their respective solutions even at concentrations higher than 50 mg/mL. When mixed together, the instantaneous mixture solutions remained transparent at concentrations from 0.1 to 5 mg/mL. Infrared spectra on the mixture at $\text{MR} = 1/2$ (i.e., equal molar ratio between COOH and NH_2 groups in the building molecules) demonstrated a complexation due to hydrogen bonding between the carboxyl groups in diacetylenic acid and the amino groups in 3-aminopropyltriethoxysilane (Figure 1). The sharp COOH stretch at 1699 cm^{-1} in the pure diacetylenic acid scan is replaced by an asymmetric COO^- bend at 1637 cm^{-1} for complexes.^{18,19} At the same time, the NH_3^+ asymmetric bending which occurs at 1580 cm^{-1} for pure 3-aminopropyltriethoxysilane shifts to 1557 cm^{-1} for the complexes. In time, however, the complex solutions became turbid, and dynamic light scattering measurements showed a concentration and time-dependent self-assembly (Figure 2). Higher concentrations were found to reach their corresponding maximum scattering intensity plateaus faster. In fact, a 5 mg/mL solution necessitated minutes while a concentration ≤ 0.1 mg/mL took days or even weeks. Two factors likely contributing to the increase of the scattering intensity in solutions are aggregate number and aggregate's mass M (reflected by the average hydrodynamic diameter, $\langle D_h \rangle$). Considering that $\langle D_h \rangle$ of the aggregate remains relatively constant during the whole period, the increase of intensity corresponds primarily to the increase of aggregate numbers in the association process.

Additional experimentation indicated that same concentrations undergo a common assembly process. Complex solutions (1 mg/mL) at $\text{MR} = 5/1$, $1/1$, and $1/2$ reached thermodynamic stability after approximately 40 min (Figure 2b). The resultant aggregates produced a spherical shape, as almost no size dependence on the scattering angles was observed. Although the assembly process and shape were consistent, the actual morphologies at

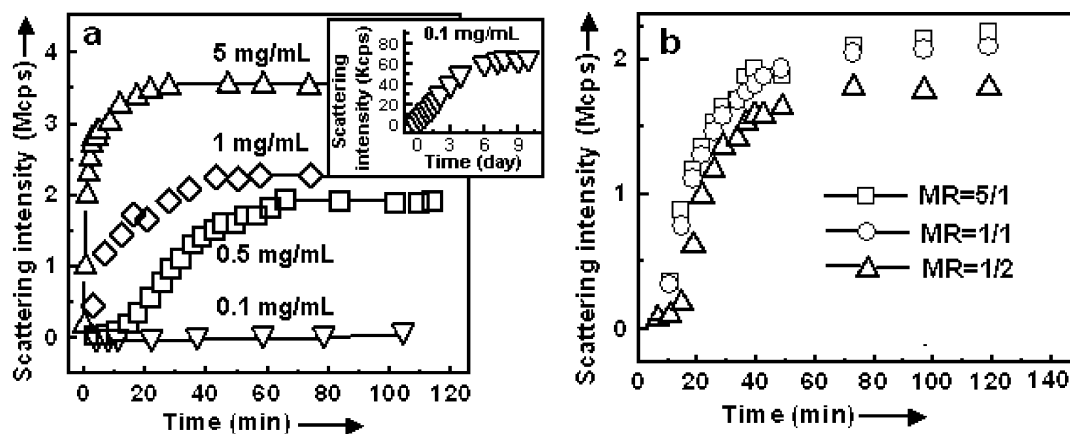


Figure 2. Dynamic light scattering characterizations of the self-assembly process for 5,7-dodecadienedioic acid/3-aminopropyltriethoxysilane complexes in THF. (a) Different concentrations at the same MR of $1/1$ (inset, the scattering intensity of the complex solution at 0.1 mg/mL versus time). (b) Different MRs at the same concentration (1 mg/mL). MR is the molar ratio between 5,7-dodecadienedioic acid and 3-aminopropyltriethoxysilane building molecules.

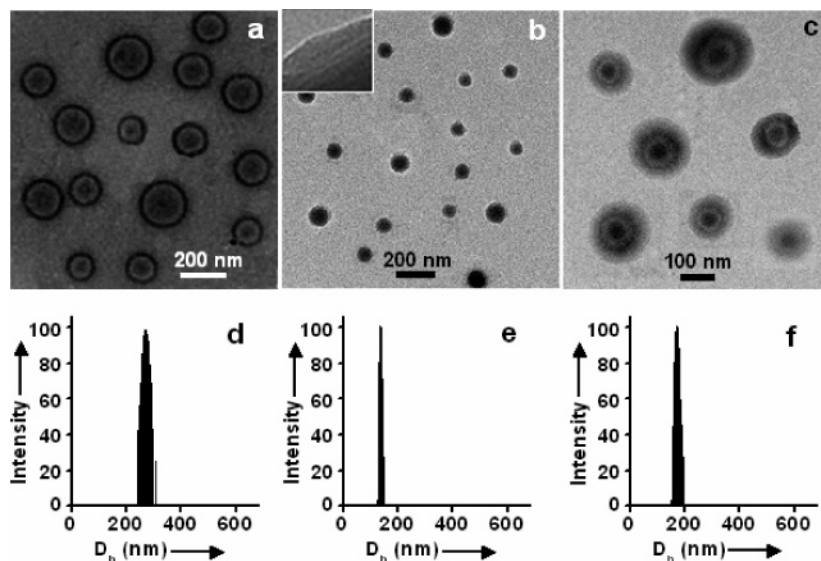


Figure 3. TEM images and dynamic light scattering measurements of the hybrid aggregates at 1 mg/mL for different MRs. (a, d) MR = 5/1; (b, e) MR = 1/1; (c, f) MR = 1/2.

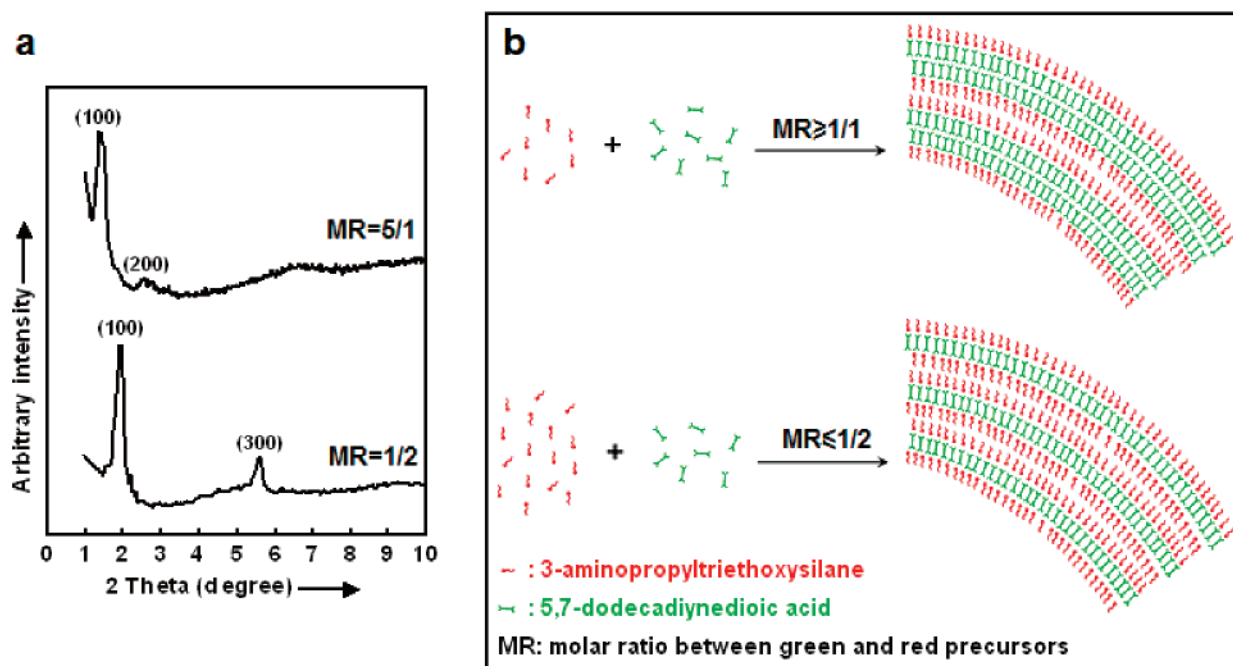


Figure 4. XRD patterns of the hybrid aggregates (a) and schematic illustration of the lamellar structure (b).

different MR values varied. Vesicles, solid spheres, and hollow spheres were observed when MR = 5/1, 1/1, and 1/2, respectively (Figure 3). The corresponding average hydrodynamic diameter of the vesicles, solid spheres and hollow spheres are 273, 140, and 170 nm, respectively, with uniform sizes (polydispersity of 0.005–0.1). Interestingly, we notice that there is a “core” in the hollow part for both vesicles and hollow spheres. To find out the “core” components, we conducted NMR measurements for the above two nanoparticle solutions at MR = 5/1 and 1/2. Almost no signal for the free precursor molecules (unconnected with another precursor molecule by hydrogen bonding) in the resultant solutions can be detected. It means that the excessive precursors are mainly in the aggregated state rather than molecularly dispersed in solution. Therefore, the “core” part may be contributed to the aggregation of excessive free precursor molecules. Similar results for self-assembly of small organic molecules have been reported.¹⁵ Figure 4a shows X-ray diffraction (XRD) patterns of the aggregates prepared at

MRs of 5/1, 1/1, and 1/2, which suggests the presence of an ordered lamellar mesostructure for vesicles and solid as well as hollow spheres with d_{100} diffractions at 6.2 and 4.8 nm, respectively. TEM (inset in Figure 3b) further confirms the ordered lamellar structure with an inter-lamellar distance of ~ 4.5 nm for a solid sphere, which agrees well with the XRD result. The different d_{100} diffractions for $\geq 1/1$ and $\leq 1/2$ are due to different repeat units (Figure 4b). For $\text{MR} \geq 1/1$, the repeat unit is composed of two 5,7-dodecadienedioic acid and two 3-aminopropyltriethoxysilane molecules; for $\text{MR} \leq 1/2$, the repeat unit includes one 5,7-dodecadienedioic acid and two 3-aminopropyltriethoxysilane molecules.

To further study the effect of MR values on the aggregate morphologies, we added excessive amount of 5,7-dodecadienedioic acid or 3-aminopropyltriethoxysilane to stable complex solutions at 1 mg/mL and MR = 1/1 to achieve final molar ratios of 5/1 and 1/2, respectively. DLS demonstrates that both the scattering intensity and average hydrodynamic diameter

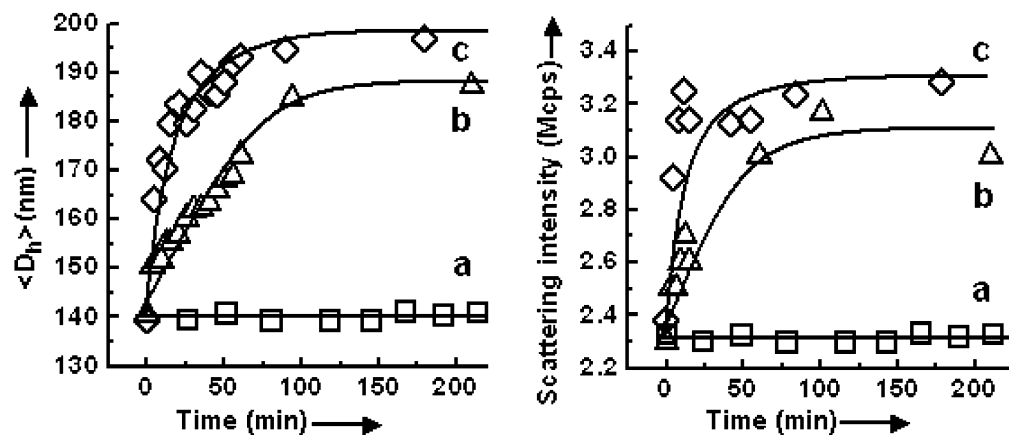


Figure 5. (a) The hybrid aggregate solution at 1 mg/mL and MR = 1/1. (b, c) More 3-aminopropyltriethoxysilane and 5,7-dodecadienedioic acid were added to a to produce the final MR values of 1/2 and 5/1, respectively.

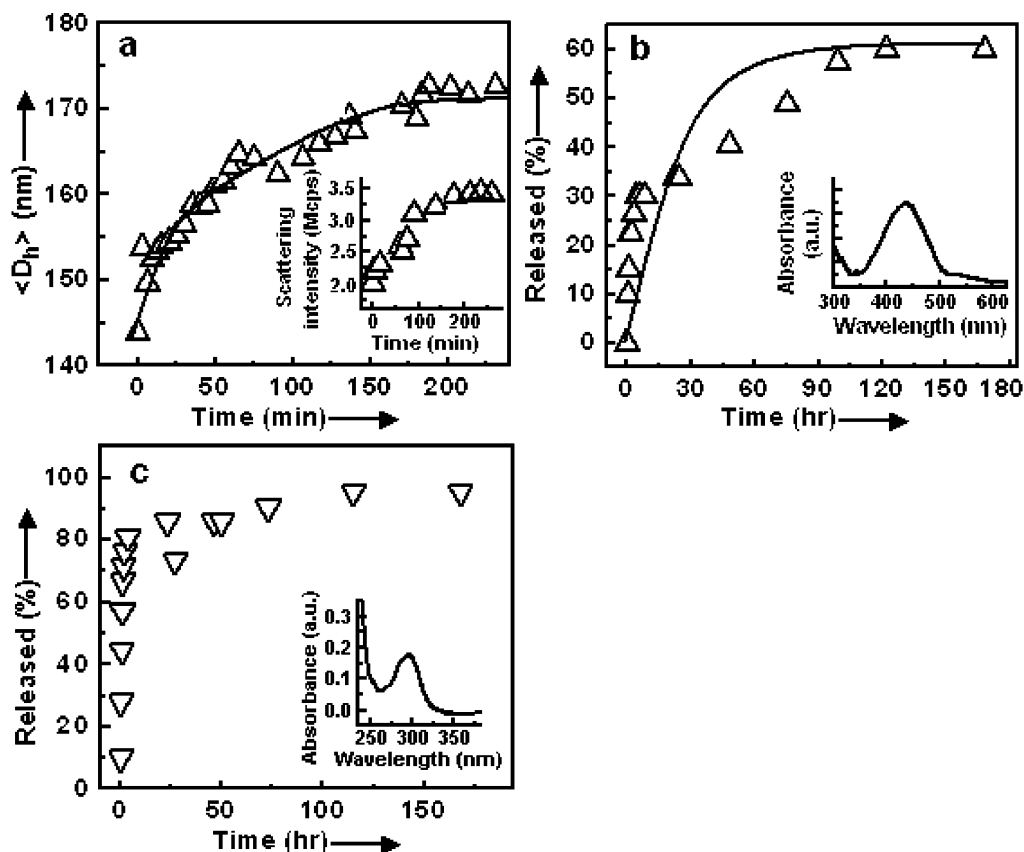


Figure 6. (a) DLS characterizations for the loading process of α -sexithiophene into the nanoparticles at 1 mg/mL and MR = 1/1 (inset, scattering intensity of the complex solution versus time). (b) UV-vis characterizations for the releasing process of above loaded α -sexithiophene at room temperature (inset, typical UV-vis spectrum of a sexithiophene-loaded nanoparticle solution). (c) UV-vis characterizations for the releasing process of an aspirin-loaded nanoparticle solution at 1 mg/mL and MR = 1/1 (inset, typical UV-vis spectrum of the aspirin-loaded nanoparticle solution).

increase and reach the equilibrium in ~ 2 h (Figure 5). TEM indicates that the final morphology for MR = 5/1 and 1/2 at equilibrium remains a solid sphere, similar to those at MR = 1/1 and only slightly larger. Eisenberg et al. reported that the multiple morphologies, as well as the dimensions, were a result of a thermodynamic equilibrium that prevailed while the aggregates were being formed during the association process.²⁰ For current system, with the addition of excess precursors, the pre-existing stable aggregates at MR = 1/1 would be expected to swell until a new thermodynamic equilibrium.

It should be noted that the complex concentration also affects the aggregate size. For a fixed MR value, DLS measurements show that the average hydrodynamic diameter increases with the rise of concentrations from 0.1 mg/mL to 1 mg/mL. For

example, the average hydrodynamic diameters with a MR value of 1/1 are 225, 181, and 140 nm at 0.1, 0.5, and 1 mg/mL, respectively. Further increase of the concentration to 5 mg/mL distinguishes the aggregate diameter variety in terms of the MR value. For MR = 1/1, the average hydrodynamic diameter keeps constant; for MR = 5/1 and 1/2, the diameter increases. To the best of our knowledge, this interesting size dependence on molar ratios has not been reported. More study is under way to investigate the detailed mechanism.

Such nanoparticles demonstrate promising applications as drug-delivery vehicles.^{14,21–25} In present work, we use α -sexithiophene as a model guest to study the loading and releasing dynamics in the aggregates. As shown in Figure 6a, with the entrance of guest molecules into the particles, the aggregate

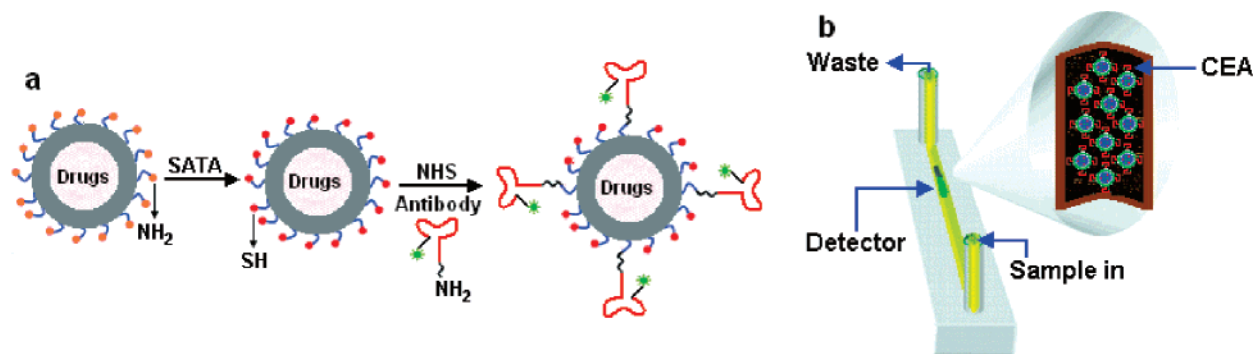


Figure 7. (a) Schematic diagram of the conjugation reaction of hybrid nanoparticles with N-succinimidyl S-acetylthioacetate (SATA), poly(ethylene glycol)- α -maleimide ω -N-hydroxysuccinimide ester (NHS-PEG-MAL), and anti-CEA antibody. (b) Labeled nanoparticles only target to silica beads modified with CEA.

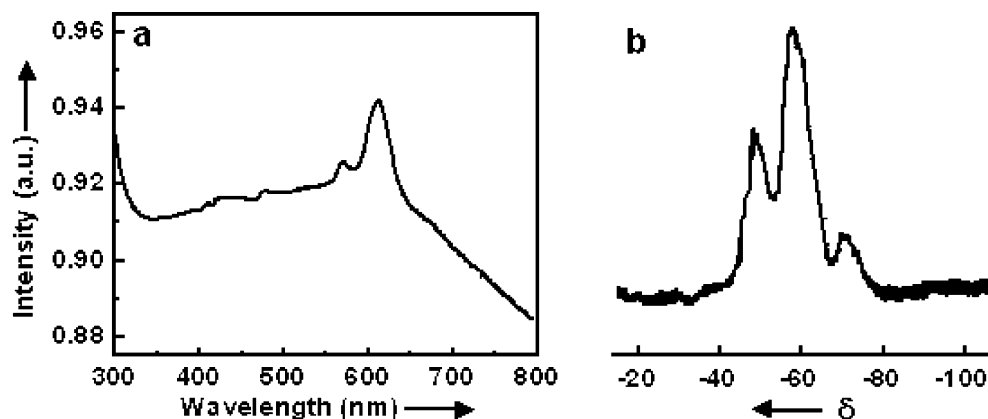


Figure 8. (a) Typical UV-vis spectrum of the hybrid aggregate solutions (1 mg/mL, MR = 1/1) after topochemical polymerization of diacetylenic moieties by exposure to UV light at wavelength of 254 nm. (b) ^{29}Si NMR spectrum of the hybrid aggregates (1 mg/mL, MR = 1/1) after hydrolysis under weak acid condition.

diameter grows and reaches the maximum value in ~ 4 h. At the same time, the scattering intensity (Figure 6a, inset) of the mixture solution also increases due to the density increase of the aggregates. Most of loaded α -sexithiophene molecules were released in 5 days at room temperature (Figure 6b). To investigate the size effect of loaded guest molecules on the releasing process, we also conducted the same experiments with a smaller molecule, aspirin. As expected, most of aspirin molecules were released to the environment in hours (Figure 6c). Similar releasing results were observed when the vesicles and hollow spheres were used.

One of the major concerns regarding drug delivery is the low therapeutic index of the drugs used.²⁶ This limitation can be partially overcome by using drugs that are specifically targeted to certain cells, such as cancer cells, without killing the surrounding noncancerous tissue.²⁷ Functional COOH or NH_2 groups on the hybrid aggregate surface can attach various labeled biomolecules, which endows the nanoparticles with potential applications as targeted drug-delivery vehicles.²⁸ To test the viability of this approach, we attached certain labels to our nanoparticles as shown in Figure 7a, and details of the test method will follow description of the labeling process. Because we are interested in developing a methodology for using antibodies to direct the delivery of hybrid nanoparticles to specific positions and know that carcinoembryonic antigen (CEA) represents a well-characterized target, we used anti-CEA antibody to generate our hybrid nanoparticle-antibody bioconjugates, again shown in Figure 7a. The hybrid nanoparticles had been prepared at 1 mg/mL and MR = 1/2 before the modification. Microchannel technology, a system in which the channels are embedded with labeled silica beads, analogous in some ways to affinity chromatography, described in other

work,^{29,30} was utilized as the target and detector (Figure 7b). To determine functional effectiveness of the labeled nanoparticles in seeking a labeled target, both of the silica beads without CEA and with anti-CEA antibody modification, as a control, were first located at the inner wall of the microchannel. After the antibody-modified hybrid nanoparticles passed through the microchannel, no drug (aspirin) signal can be detected in the above silica beads by fluorescent spectrometer. In comparison, the same experiment utilizing the CEA-modified silica beads did produce a strong drug signal. That is, the bioconjugate nanoparticles were only attached to the silica beads with CEA.

As previously discussed, collective noncovalent interactions spatially arrange the diacetylenic moiety into ordered lamellar structure that can undergo topochemical polymerization upon ultraviolet (UV) or X-ray irradiation.^{31–33} The UV-vis spectrum (Figure 8a) shows the absorption maximum at ~ 614 nm for the as-polymerized blue aggregates. In turn, the successful formation of the blue aggregates also indicates the highly ordered π - π stacking of the diacetylenic components in the assemblies. Increasing the temperature of the aggregates (> 60 °C) transits the maximum absorption to ~ 470 nm and their color from blue to red due to the change of effective conjugation length of the polydiacetylenic backbones.³² Such thermochromic hybrid aggregates are of potential interest for smart drug-delivery process and sensing materials.³³ The hybrid aggregates can also be crosslinked by hydrolysis and condensation reactions of 3-aminopropyltriethoxysilane under mild conditions.³⁴ The ^{29}Si NMR spectroscopic experiment indicates partial polycondensation of the Si-OH bonds in a weak acidic environment (Figure 8b). Three peaks are attributed to T^1 ($\delta = 51$, $\text{CSi}(\text{OH})_2(\text{OSi})$), T^2 ($\delta = 60$, $\text{CSi}(\text{OH})(\text{OSi})_2$), and T^3 signals ($\delta = 69$,

CSi(OSi)₃, respectively, where T^1 is the level of condensation at a particular center. No signal from T^0 ($\delta = 41.5$, CSi(OH)₃) is observed, i.e., each silicon atom is linked by at least one Si–O–Si bond to the others. The relative intensity of the $T^1/T^2/T^3$ signals is 3/5/1 and corresponds to an overall polycondensation of 60%. Obviously, a fully condensed system is difficult to achieve in this case due to the slow diffusion of water into the hybrid nanoparticle. The interparticle condensation reaction does occur for present system at 1 mg/mL, which can be prevented by diluting the precursor nanoparticle solution.³⁵ The crosslinked stable nanoparticles possess wider applications in numerous fields, including drug delivery.^{36,37}

On the basis of our experimental observations and previous studies,³² we believe that a collective effect of noncovalent interactions, such as the hydrogen bonding between 5,7-dodecadienedioic acid and 3-aminopropyltriethoxysilane and the π - π stacking of the diacetylenic moieties, is responsible for the formation of such hierarchical assemblies. Since hydrogen bonds at present system are immediately formed upon mixed of two building molecules, the main driving force for the unusual slow association is that the close packing of building complexes takes time.³² Figure 4b further indicates that, during the cooperative assembly process, the diacetylenic units within the complexes were spatially arranged in a polymerizable fashion and topochemically polymerized upon UV irradiation, creating the blue polydiacetylenic aggregates containing the ene-yne alternating chains.³² Deriving a clear mechanism for this unusual slow assembly, however, is still a challenge. Additional studies are underway to investigate the mechanism and how the MR affects the mesostructure and morphology.

Conclusion

In summary, we have studied the aggregation of two polymerizable precursors in their common solvent. Diacetylenic π - π stacking in the complex drives the self-assembly and the association process strongly depends on the complex concentration: higher concentrations speed up the association process dramatically. This phenomenon has not been reported for the self-assembly of organic molecules. Additionally, the complex assembles into aggregates with controlled morphologies from vesicles to solid spheres and hollow spheres by altering the molar ratio of two precursors. While it seems that the self-assembly in this case is expectable, the unusual association process and formation of different morphologies are unique. After modification with anti-CEA antibody on the aggregate surface, the hybrid nanoparticles only target to specific positions with CEA, demonstrating great potential applications as targeted drug-delivery vehicles. As-synthesized hybrid nanoparticles can be further stabilized by ready intraparticle crosslinking reactions of either precursor. Particularly, the derived polydiacetylenic aggregates demonstrate a thermochromatic property and may be applied as sensing materials. Those novel phenomena, along with the simplicity in the preparation of aggregates, make the system promising in addressing related theoretical problems and practical applications.

Acknowledgment. This work is partially supported by the LANL Director's Fellowship. The author thanks Dr. Dean E. Peterson and Dr. Liangde Lu for the suggestive discussion.

References and Notes

- (1) Chen, D.; Jiang, M. *Acc. Chem. Res.* **2005**, *38*, 494–502.
- (2) Savic, R.; Luo, L.; Eisenberg Maysinger, A. D. *Science* **2003**, *300*, 615–618.
- (3) Shchukin, D. G.; Kohler, K.; Mohwald, H.; Sukhorukov, G. B. *Angew. Chem., Int. Ed.* **2005**, *44*, 3310–3314.
- (4) Bronich, T. K.; Ouyang, M.; Kabanov, V. A.; Eisenberg, A.; Szoka, F. C., Jr.; Kabanov, A. V. *J. Am. Chem. Soc.* **2002**, *124*, 11872–11873.
- (5) Kabanov, A. V.; Bronich, T. K.; Kabanov, V. A.; Yu, K.; Eisenberg, A. *J. Am. Chem. Soc.* **1998**, *120*, 9941–9942.
- (6) Shchukin, D. G.; Sukhorukov, G. B.; Mohwald, H. *Angew. Chem., Int. Ed.* **2003**, *42*, 4472–4475.
- (7) Duan, H.; Chen, D.; Jiang, M.; Gan, W.; Li, S.; Wang, M.; Gong, J. *J. Am. Chem. Soc.* **2001**, *123*, 12097–12098.
- (8) Fujii, S.; Cai, Y.; Weaver, J. V. M.; Armes, S. P. *J. Am. Chem. Soc.* **2005**, *127*, 7304–7305.
- (9) Peng, H.; Chen, D.; Jiang, M. *Macromolecules* **2005**, *38*, 3550–3553.
- (10) Qi, K.; Ma, Q.; Remsen, E. E.; Clark, C. G., Jr.; Wooley, K. L. *J. Am. Chem. Soc.* **2004**, *126*, 6599–6607.
- (11) Caruso, F.; Caruso, R. A.; Mohwald, H. *Science* **1998**, *282*, 1111–1114.
- (12) Chen, D.; Peng, H.; Jiang, M. *Macromolecules* **2003**, *36*, 2576–2578.
- (13) Horbaschek, K.; Hoffmann, H.; Hao, J. C. *J. Phys. Chem. B* **2000**, *104*, 2781–2784.
- (14) Liu, Z.; Chen, G.; Dunphy, D. R.; Jiang, Y.-B.; Assink, R. A.; Brinker, C. J. *Angew. Chem., Int. Ed.* **2003**, *42*, 1731–1734.
- (15) Peng, H.; Chen, D.; M. Jiang, *J. Phys. Chem. B* **2003**, *107*, 12461–12464.
- (16) Peng, H.; Chen, D.; M. Jiang, *Langmuir* **2003**, *19*, 10989–10922.
- (17) Kumar, R.; Chen, M.-H.; Parmar, V. S.; Samuelson, L. A.; Kumar, J.; Nicolosi, R.; Yoganathan, S.; Watterson, A. C. *J. Am. Chem. Soc.* **2004**, *126*, 10640–10644.
- (18) Tachibana, H.; Yamanaka, Y.; Sakai, H.; Abe, M.; Matsumoto, M. *Thin Solid Films* **2001**, *382*, 257–262.
- (19) Tachibana, H.; Yamanaka, Y.; Sakai, H.; Abe, M.; Matsumoto, M. *Colloids Surf., A* **2002**, *198–200*, 83–88.
- (20) Zhang, L.; Eisenberg, A. *Science* **1995**, *268*, 1728–1731.
- (21) Bellomo, E. G.; Wyrsta, M. D.; Pakstis, L.; Pochan, D. J.; Deming, T. J. *Nat. Mater.* **2004**, *3*, 244–248.
- (22) Dou, H.; Jiang, M.; Peng, H.; Chen, D.; Hong, Y. *Angew. Chem., Int. Ed.* **2003**, *42*, 1516–1519.
- (23) Gao, C.; Donath, E.; Mohwald, H.; Shen, J. *Angew. Chem., Int. Ed.* **2002**, *41*, 3789–3793.
- (24) Jenekhe, S. A.; Chen, X. L. *Science* **1998**, *279*, 1903–1907.
- (25) Moffit, M.; Khougaz, K.; Eisenberg, A. *Acc. Chem. Res.* **1996**, *29*, 95–102.
- (26) Leamon, C. P.; Low, P. S. *Drug Discov. Today* **2001**, *6*, 44–51.
- (27) Nayak, S.; Lee, H.; Chmielewski, J.; Lyon, L. A. *J. Am. Chem. Soc.* **2004**, *126*, 10258–10259.
- (28) Farokhzad, O. C.; Jon, S.; Khademhosseini, A.; Tran, T. T.; LaVan, D. A.; Langer, R. *Cancer Res.* **2004**, *64*, 7668–7672.
- (29) Wen, X.; Wu, Q.; Lu, Y.; Fan, Z.; Charnsangavej, C.; Wallace, S.; Chow, D.; Li, C. *Bioconjugate Chem.* **2001**, *12*, 545–553.
- (30) Buranda, T.; Huang, J.; Perez-Luna, V. H.; Schreyer, B.; Sklar, L. A.; Lopez, G. P. *Anal. Chem.* **2002**, *74*, 1149–1156.
- (31) Lkada, S.; Peng, S.; Spevak, W.; Charych, D. *Acc. Chem. Res.* **1998**, *31*, 229–239.
- (32) Peng, H.; Lu, Y. *Langmuir* **2006**, *22*, 5525–5527.
- (33) Peng, H.; Tang, J.; Pang, J.; Chen, D.; Yang, L.; Ashbaugh, H. S.; Brinker, C. J.; Yang, Z.; Lu, Y. *J. Am. Chem. Soc.* **2005**, *127*, 12782–12783.
- (34) Peng, H.; Tang, J.; Yang, L.; Pang, J.; Ashbaugh, H. S.; Brinker, C. J.; Yang, Z.; Lu, Y. *J. Am. Chem. Soc.* **2006**, *128*, 5304–5305.
- (35) Thurmond, K. B.; Kowalewski, T.; Wooley, K. L. *J. Am. Chem. Soc.* **1997**, *119*, 6656–6665.
- (36) Brown, G. O.; Bergquist, C.; Ferm, P.; Wooley, K. L. *J. Am. Chem. Soc.* **2005**, *127*, 11238–11239.
- (37) Fujii, S.; Cai, Y.; Weaver, J. V. M.; Armes, S. P. *J. Am. Chem. Soc.* **2005**, *127*, 7304–7305.